

# Preparation of the $\text{Cd}_{1-x}\text{Zn}_x\text{Se}$ alloys in the nanophase form using microwave irradiation

H. Grisaru,<sup>a</sup> O. Palchik,<sup>a</sup> A. Gedanken,<sup>\*a</sup> V. Palchik,<sup>b</sup> M. A. Slifkin<sup>b</sup> and A. M. Weiss<sup>b</sup>

<sup>a</sup>Department of Chemistry, Bar-Ilan University, Ramat-Gan 52900, Israel.

E-mail: [gedanken@mail.biu.ac.il](mailto:gedanken@mail.biu.ac.il)

<sup>b</sup>Department of Electronics, Jerusalem College of Technology, Jerusalem 91160, Israel

Received 24th July 2001, Accepted 30th October 2001

First published as an Advance Article on the web 3rd January 2002

Nanoparticles of the  $\text{Cd}_{1-x}\text{Zn}_x\text{Se}$  alloy with different stoichiometries ( $x = 0.1, 0.2, 0.3$ ) have been prepared using the microwave-assisted polyol method. In this simple and quick reaction the polyol (ethylene glycol) is both the solvent and the reducing agent. XRD studies show that nanoparticles are formed in the wurtzite (hexagonal) form with an average diameter of the nanocrystals of 5–8 nm. Electron microscopy studies show that these particles form monodisperse spherical aggregates with a diameter of approximately 200 nm. Electronic properties of the as-prepared alloys have been studied using photoacoustic spectroscopy (PAS). Also, the particles have been characterized using TGA, DSC, XPS and EDS analysis. The results of these studies are presented in this paper.

## Introduction

Interest in optical devices that can operate in the visible spectrum has motivated recent research in group II–VI wide band-gap semiconducting materials.<sup>1</sup> These compounds are particularly attractive because their optical properties can be tailored to the requirements of various photonic devices.<sup>2</sup> CdSe and ZnSe are well studied binary semiconductors with band gaps of 1.73 and 2.58 eV, respectively, and diverse structural properties.<sup>3</sup> Their electronic properties can be varied within the 1.73–2.58 eV range by mixing them in order to form a pseudo-binary CdSe–ZnSe alloy. This band gap range is used for devices such as radiation detectors, lasers and color TVs.<sup>2,4,5</sup> Usually, these materials are prepared using vacuum techniques, but recently, electrochemical methods, which are much simpler and cheaper than the cost-intensive vapor process,<sup>6</sup> have been developed. No other soft chemistry routes have been used for synthesis of these materials. To the best of our knowledge the microwave-assisted synthesis is the first 'chimi-douce' preparation used for the pseudo-binary alloy Cd–Zn–Se.

The polyol method was developed over the past two decades and has been applied to the preparation of submicrometer nanoparticles of the easily reducible transition metals.<sup>7</sup> This method is based on alcohols (such as ethylene glycol, but other glycols can be used as well) acting as reducing agents of metallic cations to form the corresponding metals. In almost all reactions, the polyol plays the role of the solvent for the same reaction. Generally, the solution reactions for the formation of binary chalcogenides are relatively slow,<sup>8</sup> and are conducted under hydro- or solvo-thermal conditions in special high temperature and pressure equipment in order to accelerate their rate. Even under these conditions the reaction proceeds for many hours or even days.<sup>9</sup>

Recently, we have found that the application of microwave radiation or ultrasound greatly facilitates the use of the polyol method for the preparation of binary chalcogenides (selenides and tellurides).<sup>10</sup> In most experiments, the microwave reaction is completed within few minutes, the maximum duration being one hour.

The application of microwaves in inorganic chemistry began only in the late 1980s.<sup>11</sup> Ethylene glycol (and other glycols) is an excellent susceptor of microwave radiation because of its

high permanent dipole. This is important because ethylene glycol is a good reducing agent only at high temperature. The metallic particles that are produced as intermediates in the polyol reaction are also good susceptors of microwave radiation. This causes rapid heating of these particles. While the solvent temperature will be close the boiling point of ethylene glycol, it is likely that the temperature in the reaction cell will be much higher than the surrounding liquid. Whittaker and Mingos<sup>12</sup> recently reported that high boiling point alcohols are superior solvents in microwave-assisted reactions because they help prevent arcing, which is known to lead to the decomposition of solvents, resulting in carbon and carbonaceous residues. Arcing is considered the main source of the high level of impurities, which are found in the end product. In the current report, the microwave-assisted polyol method is shown to be an excellent method for the preparation of the  $\text{Cd}_{1-x}\text{Zn}_x\text{Se}$  alloys. Preliminary results with regard to basic ethylene glycol solution have been reported.<sup>13</sup>

## Experimental

All reagents were of highest commercially available purity. Elemental Se, cadmium acetate, zinc acetate and ethylene glycol were purchased from Aldrich Co., and used without further purification. The X-ray diffraction patterns of the products were recorded with a Bruker AXS D8 Advance Powder X-ray Diffractometer (using  $\text{CuK}\alpha$   $\lambda = 1.5418 \text{ \AA}$  radiation). Peak fitting and lattice parameter refinement were computed using the Topas and Metric programs (Bruker Analytical X-Ray Systems). EDS measurements were done on an X-ray microanalyzer (Oxford scientific) built on a JSM-840 Scanning Electron Microscope (JEOL). The transmission electron micrographs (TEM) were imaged on a JEOL-JEM 100SX microscope, using a 100 kV accelerating voltage. High resolution TEM (HRTEM) images were taken using a JEOL-3010 with 300 kV accelerating voltage. A conventional monochrome CCD camera, with resolution of  $768 \times 512$  pixels, was used to digitize the images. The digital images were processed with the Digital Micrograph software package (Gatan, Inc., Pleasanton, CA, USA). HRTEM image analysis and electron diffraction indexing were performed using the EMS package.<sup>14</sup> Samples for TEM were prepared by placing a drop of the

sample suspension on a copper grid (400 mesh, Electron Microscopy Sciences) coated with carbon film. The grid was then air-dried.

Elemental analysis (carbon) was done with an EA 1110 CHNS-O elemental analyzer. Differential scanning calorimetric analysis (DSC) was carried out on a Mettler Toledo TC 15. Thermogravimetric analysis (TGA) was done on a Mettler Toledo TGA/SDTA851. For both DSC and TGA, nitrogen or argon served as the purging gas, and the scanning rate was  $5\text{ }^{\circ}\text{C min}^{-1}$ . X-Ray photoelectron spectra (XPS) were recorded using an AXIS, HIS, 165, ULTRA (Kratos Analytical, Inc.).

The electronic properties of the nanoparticles were measured using photoacoustic spectroscopy (PAS). Photoacoustic measurements were conducted employing a home-made instrument which has been described elsewhere.<sup>15</sup> The signals, which are acquired as a function of wavelength, were normalized against the absorption of carbon black powder, the 100% absorber. The band gap is calculated by the 'knee' method for all the samples.<sup>16</sup>

Microwave-assisted reactions were carried out in a Spectra-900 W microwave oven, with a 2.45 GHz working frequency. The oven was modified to include a refluxing system. In all experiments, the microwave oven was cycled as follows: on for 21 s, off for 9 s, with total power always at 900 W. This cycling mode was chosen in order to reduce the risk of superheating the solvent. All reactions were conducted under flowing nitrogen.

### Microwave synthesis

Zinc and cadmium acetate (in stoichiometric quantities) were dissolved in ethylene glycol (50 ml) by gently heating in the microwave oven for approximately one minute. Then, a stoichiometric quantity of Se powder (0.079 g) was added. The system was purged for few minutes with nitrogen and then the microwave oven was cycled for 1 h under nitrogen. In the post-reaction treatment, the product was centrifuged once with the mother liquid, and a few times with EtOH, at  $20\text{ }^{\circ}\text{C}$  and 9000 rpm. The product was then dried overnight under vacuum. The samples were annealed under nitrogen for 12 h at  $550\text{ }^{\circ}\text{C}$ .

## Results and discussion

### Powder XRD studies

Fig. 1a–c shows the X-ray diffraction patterns for all of the alloy compositions, which were synthesized. In each case, the polycrystalline hexagonal (wurtzite) structure was obtained (Powder diffraction file, PDF #08-0459). This result is consistent with previously published data showing that alloys with  $x < 0.5$  have a hexagonal wurtzite structure.<sup>9,17</sup> Small diffraction peaks which are attributed to unreacted Se were also detected (PDF #06-0362). The Se peaks are marked by an asterisk in Fig. 1a–d. The very broad peaks indicate that the products are nanosized. The nanocrystal diameter was calculated with the Debye–Scherrer (DS) equation,<sup>18</sup> and was found to be in the range of 5–8 nm. The calculated sizes for all of the samples are given in Table 1.

The bulk composition of the as-prepared compounds was obtained from EDS measurements, and the results are shown in Table 1. The compositions of the resulting alloys are relatively close to the initial ratios of the constituent elements introduced into the solution. This result demonstrates our ability to control the stoichiometry of the  $\text{Cd}_{1-x}\text{Zn}_x\text{Se}$  alloy by controlling the ratio of the reacting salts. For all as-prepared samples, background diffraction is observed in the PXRD data. The presence of such a background might indicate the formation of an amorphous product.

The composition of the alloy did not change after heating the product to  $550\text{ }^{\circ}\text{C}$ , but the percentage of Se in the samples was

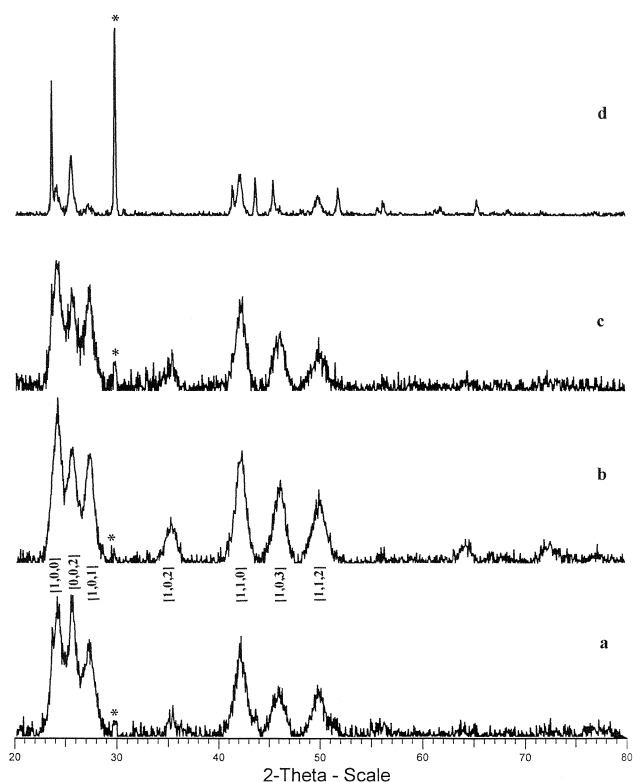


**Fig. 1** Powder XRD patterns of as-prepared (a–c) hexagonal  $\text{Cd}_{1-x}\text{Zn}_x\text{Se}$  alloys prepared by microwave heating: (a) for  $\text{Cd}_{0.9}\text{Zn}_{0.1}\text{Se}$ ; (b) for  $\text{Cd}_{0.8}\text{Zn}_{0.2}\text{Se}$ ; (c) for  $\text{Cd}_{0.7}\text{Zn}_{0.3}\text{Se}$ ; (d) hexagonal  $\text{CdSe}$  for the initial stoichiometry of  $\text{Cd}_{0.8}\text{Zn}_{0.2}\text{Se}$  prepared by regular (reflux) heating for 24 h (control experiment).

reduced from 4 to *ca.* 0.2%, probably as a result of evaporation of the unreacted Se.

The diameter of the annealed samples increased to 37–45 nm for all samples, as calculated by the DS equation.

In order to compare regular and microwave-heated reactions, parallel control experiments were carried out under identical conditions, but without microwave irradiation, using regular reflux. These control experiments were conducted for 24 h, and their typical PXRD spectrum is shown in Fig. 1d. The major contribution to these PXRD spectra is from unreacted Se. Diffraction peaks related to hexagonal  $\text{CdSe}$  are also present for the initial stoichiometry of  $\text{Cd}_{0.8}\text{Zn}_{0.2}\text{Se}$ . EDS measurements of the products show that almost no Zn is incorporated in non-microwave-assisted control reactions. The results of the control reactions provide further evidence of the superiority of microwave over regular heating.

### Electron microscopy studies: TEM, HR-TEM and SEM

TEM micrographs of the as-prepared and heated alloys with  $x = 0.1$ – $0.3$  are shown in Fig. 2a–f. These figures show that the nanoparticles of these alloys are monodispersed nanospheres, with low aggregation, and having an average diameter of 195 nm which is independent of  $x$  (Fig. 2a, b, d, f). Closer examination of the nanospheres reveals differences in their morphologies. For the  $x = 0.3$  alloy, the morphology of the

**Table 1** The dimensions of the produced particles as measured by various methods

| Product                                   | Dimensions from XRD/nm (as-prepared) | EDS stoichiometry                           | PAS band gap/eV (as-prepared) |
|---|--------------------------------------|---|-------------------------------|
| $\text{Cd}_{0.9}\text{Zn}_{0.1}\text{Se}$ | 6.9                                  | $\text{Cd}_{0.85}\text{Zn}_{0.15}\text{Se}$ | 1.97                          |
| $\text{Cd}_{0.8}\text{Zn}_{0.2}\text{Se}$ | 7.5                                  | $\text{Cd}_{0.74}\text{Zn}_{0.26}\text{Se}$ | 2.05                          |
| $\text{Cd}_{0.7}\text{Zn}_{0.3}\text{Se}$ | 5.9                                  | $\text{Cd}_{0.65}\text{Zn}_{0.35}\text{Se}$ | 2.10                          |

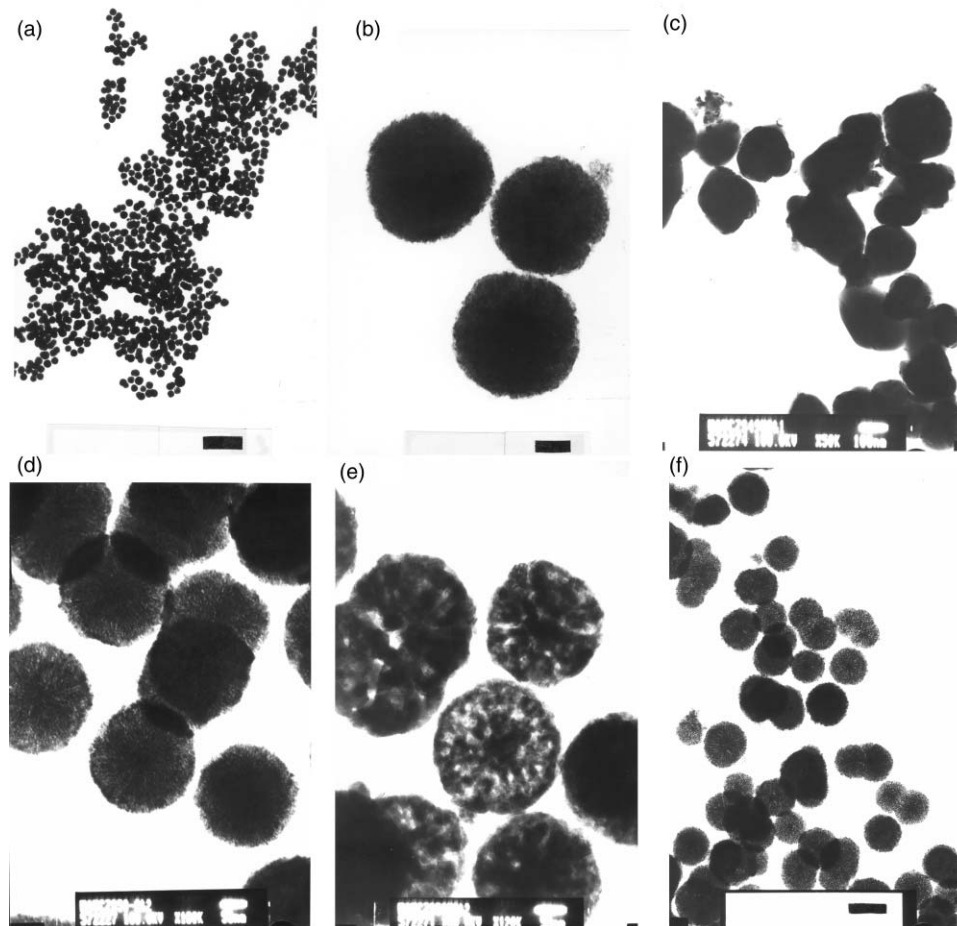


**Fig. 2** TEM pictures of (a) as-prepared  $\text{Cd}_{0.9}\text{Zn}_{0.1}\text{Se}$  (scale bar = 1  $\mu\text{m}$ ); (b) same as (a) but with higher magnification (bar = 55 nm); (c) heated  $\text{Cd}_{0.9}\text{Zn}_{0.1}\text{Se}$  (bar = 100 nm); (d) as-prepared  $\text{Cd}_{0.8}\text{Zn}_{0.2}\text{Se}$  (bar = 50 nm); (e) heated  $\text{Cd}_{0.8}\text{Zn}_{0.2}\text{Se}$  (bar = 50 nm); (f) as-prepared  $\text{Cd}_{0.7}\text{Zn}_{0.3}\text{Se}$  (bar = 200 nm).

particle is worm-like, with almost no difference between the core and the shell of the particle (Fig. 2f). The TEM picture shows a fractal spreading of the branches originating at the core and spreading to the outside. The particles retained their spherical shape after heating, and remained loosely aggregated. The average diameter of the particles after heating (160 nm) was smaller than that of the as-prepared alloy (195 nm). The internal structure of the particles also changed after heating, and they appear to be built up from smaller rounded nanocrystals with an average diameter of 40 nm. This may be due to recrystallization and growth of the smaller nanocrystals to form the bigger one as a result of the heating.

The shape of the as-prepared nanoparticles of the  $\text{Cd}_{0.8}\text{Zn}_{0.2}\text{Se}$  and  $\text{Cd}_{0.9}\text{Zn}_{0.1}\text{Se}$  alloys are very similar to that of  $\text{Cd}_{0.7}\text{Zn}_{0.3}\text{Se}$ . The only difference is that the spheres of the  $\text{Cd}_{0.8}\text{Zn}_{0.2}\text{Se}$  and  $\text{Cd}_{0.9}\text{Zn}_{0.1}\text{Se}$  alloys appear denser, with a clearly resolved core and shell. After heating, the morphologies of all three alloys are very similar. The SEM micrograph for  $\text{Cd}_{0.8}\text{Zn}_{0.2}\text{Se}$  (Fig. 3) is consistent with the results of the TEM measurements. Spherical, monodispersed, non-aggregated nanoparticles are observed for all three alloys.

The PXRD patterns of the as-prepared compounds exhibit very broad peaks, which correspond to particle sizes of a few nanometers. However, the TEM and SEM results appear to contradict the PXRD results. In order to resolve the inconsistency of the TEM and PXRD results, HR-TEM measurements were done. A representative HR-TEM image of the as-prepared  $\text{Cd}_{0.7}\text{Zn}_{0.3}\text{Se}$  alloy is shown in Fig. 4. The HR-TEM images show that the 195 nm diameter spherical aggregates actually consist of smaller nanocrystals with an average diameter of 4.5 nm. Some amorphous matrix is found to surround every  $\text{Cd}_{1-x}\text{Zn}_x\text{Se}$  cluster. This supports the

PXRD measurements, which demonstrate that the products always include both crystalline and amorphous phases with the same stoichiometry ('raisins in the cake' structure). The amorphous phase has a 'glue-like' function, holding  $\text{Cd}_{1-x}\text{Zn}_x\text{Se}$  nanocrystals together.

#### TGA and DSC measurements

The TGA measurements always show two similar mass losses (data not shown). The first loss is *ca.* 3.5–5%, and occurs at temperatures less than 120 °C. It is attributed to the presence of the some adsorbed carbonaceous species (see also XPS section). This hypothesis was confirmed by elemental analysis for carbon, which was found to be in the range of 3.5–4.5%. A second mass decrease of 3–4% is observed over the range 220–300 °C. This loss is attributed to evaporation of unreacted Se

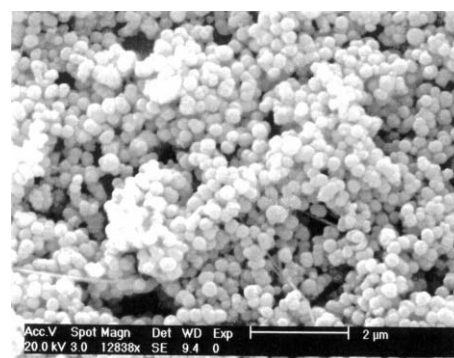


**Fig. 3** SEM image of the as-prepared  $\text{Cd}_{0.8}\text{Zn}_{0.2}\text{Se}$  alloy (scale bar = 2  $\mu\text{m}$ ).

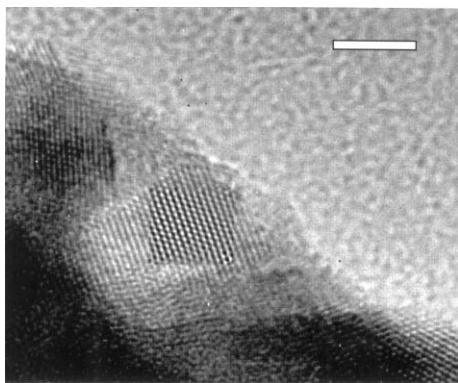


**Fig. 4** HR-TEM image of the as-prepared  $\text{Cd}_{0.7}\text{Zn}_{0.3}\text{Se}$  alloy (scale bar = 2.2 nm).

(due to the high vapor pressure of the Se). Unreacted Se is also observed in the XRD measurements. A representative example of the DSC measurements for  $\text{Cd}_{0.7}\text{Zn}_{0.3}\text{Se}$  is shown in Fig. 5. In every case, we observed a very strong and broad exothermic peak at  $340^\circ\text{C}$ , which disappears after a second heating cycle. This phenomenon may be explained as an amorphous–crystalline transition which occurs during the heating. The presence of this exothermic peak provides more evidence for the existence of an amorphous phase, which crystallizes during heating. Once crystallization occurs, this exothermic peak disappears. Very small endothermic peaks, which are observed for all compounds at *ca.*  $220^\circ\text{C}$ , are due to melting of unreacted Se. The carbon content of the samples heated to  $90^\circ\text{C}$  under nitrogen or argon was determined by elemental analysis. The average amount of C after the annealing process is 0.0138%. This is a very low level of carbon. It confirms our suggestion that the source of the carbon is surface impurities (probably solvent molecules).

#### Photoacoustic measurements (PAS)

The PAS spectra of all as-prepared alloys are shown in Fig. 6. The band gaps of the as-prepared alloys are always blue-shifted relative to the heated samples (data not shown). All of the measured band-gaps were compared with published values and with CdSe prepared in our previous studies.<sup>3,19</sup> One of the advantages of  $\text{Cd}_{1-x}\text{Zn}_x\text{Se}$  alloys is that the band gap can be modified by varying the stoichiometry of the product. Conversely, the elemental composition may be determined from the optical absorption data.<sup>6</sup> In the case of  $\text{Cd}_{1-x}\text{Zn}_x\text{Se}$  alloys, a plot of the band gap as a function of composition should produce a straight line.<sup>20</sup> A plot of the PAS-measured band gaps for the as-prepared samples *versus* composition is shown in Fig. 7, together with a theoretical curve. The line obtained for as-prepared nanoparticles is approximately

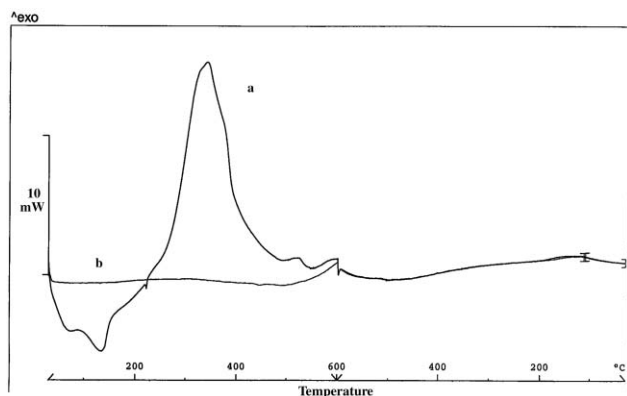


**Fig. 5** DSC patterns of the as-prepared  $\text{Cd}_{0.7}\text{Zn}_{0.3}\text{Se}$  alloy: (a) first cycle; (b) second cycle.

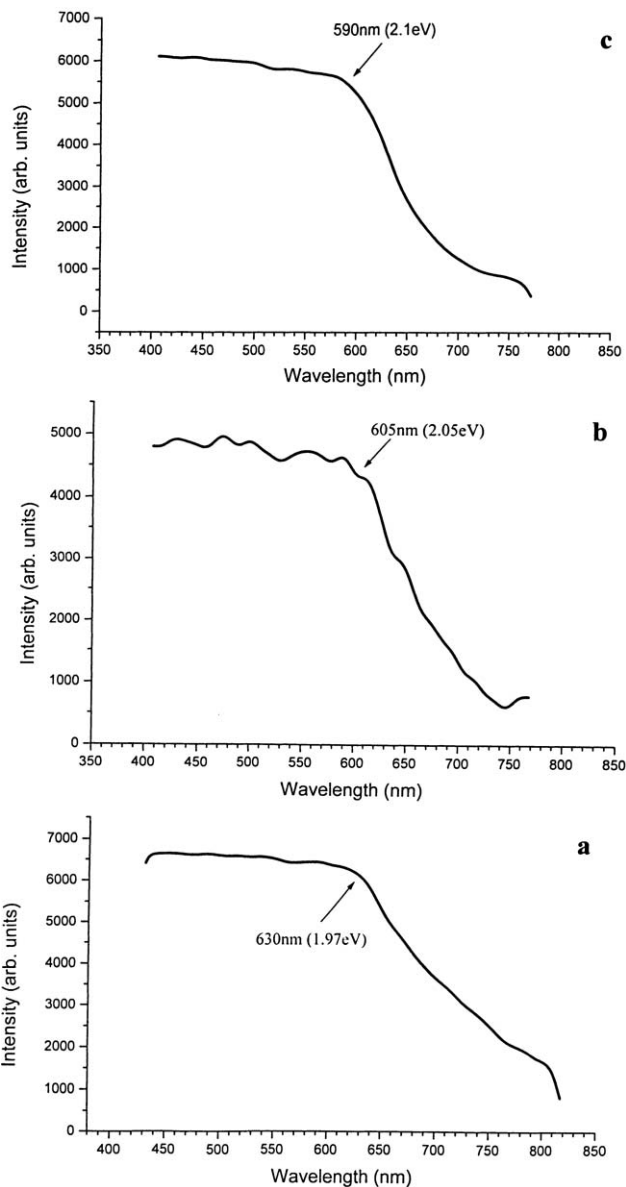


**Fig. 6** Photoacoustic measurements of the as-prepared  $\text{Cd}_{1-x}\text{Zn}_x\text{Se}$  alloys: (a) for  $\text{Cd}_{0.9}\text{Zn}_{0.1}\text{Se}$  (energy gap  $E_g = 1.97$  eV, 630 nm); (b) for  $\text{Cd}_{0.8}\text{Zn}_{0.2}\text{Se}$  ( $E_g = 2.05$  eV, 605 nm); (c) for  $\text{Cd}_{0.7}\text{Zn}_{0.3}\text{Se}$  ( $E_g = 2.10$  eV, 590 nm).

0.25 eV higher than the theoretical curve for bulk alloys, which we attribute to size quantization.<sup>21</sup> Because the theoretical band gap line is almost parallel to the measured

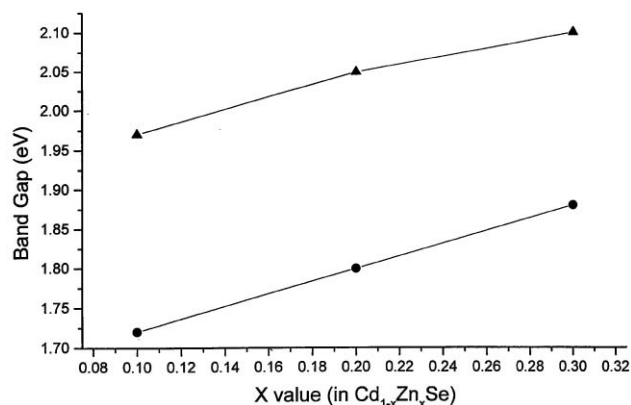


**Fig. 7** Band gap (eV) obtained from experimental and theoretical calculations for as-prepared samples *versus*  $x$  value (in  $\text{Cd}_{1-x}\text{Zn}_x\text{Se}$ ): ● theoretical  $E_g$  (eV); ▲ experimental  $E_g$  (eV).

line of the as-prepared compound, it is impossible to correlate composition to the band gap. In the case of a heated sample this is not a problem, because after heating the particles are relatively large, so the blue shift must be very small, and the band gap for such crystals will be relatively close to that of the bulk. Elemental and EDS measurements were made in order to relate band gaps obtained from the PAS measurements to stoichiometries. These results are shown in Table 1.

### XPS studies

XPS analysis was used to study stoichiometry and surface concentration of the elements in the nanoparticles. Peaks related to Cd ( $Cd_{3d}$  doublet at 403.3 and 410 eV), Zn ( $Zn_{3p}$  singlet at 87.4 eV) and Se ( $Se_{3d}$  singlet at 52.5 eV) were found at energies which are in agreement with literature data.<sup>22</sup> Peaks for carbon and oxygen were also observed, and we ascribe them to organic impurities adsorbed on the surface of the powders due to solvent decomposition. XPS spectra of the heated samples showed the same peaks as the as-prepared samples, but the ratio of the elements was slightly altered. After heating, the quantity of Se always fell, and this is consistent with the presence of unreacted Se, which evaporates during heating. The ratio of Cd:Zn was unchanged after heating (the difference was within the error range of the XPS method, which is ca. 10%).<sup>23</sup> Also, the elemental ratio determined with XPS was very close to that obtained from EDS measurements. These results lead us to conclude that true  $Cd_{1-x}Zn_xSe$  alloys were prepared, as opposed to some kind of CdSe–ZnSe core–shell, or other concentration-gradient structure. The XPS measurements are summarized in Table 2.

The main question regarding the preparation of  $Cd_{1-x}Zn_xSe$  alloys is the mechanism of their formation. In our previous work, we developed a simple method for the synthesis of nanosized binary chalcogenides (tellurides or selenides).<sup>10,19</sup> Binary chalcogenides were prepared *via* a glycol solution (like ethylene glycol), the reactants being a metallic ion and the elemental chalcogenide. We proposed a two-step mechanism for this reaction, where the first step is the reduction of the metallic ion to the corresponding metallic state. This hypothesis is based on the observation that in the absence of the elemental chalcogenide, pure metallic material is obtained. In the second step, these small metallic particles continue to absorb microwave radiation, and reduce the elemental chalcogenide.

Our attempts to prepare ZnSe from  $Zn^{+2}$  by employing this method have failed (ZnO was obtained instead). Other groups employing the regular heating (reflux) polyol method,<sup>24</sup> also failed to synthesize ZnSe. We therefore propose that in all of our samples  $Zn^{+2}$  does not undergo a reaction, but is incorporated into the ternary selenide. Since elemental Zn is not obtained in the absence of the chalcogenide, it is clear that the  $Zn^{+2}$  is not being reduced in the first stage. On the other hand, unlike the  $Zn^{+2}$ , the  $Cd^{+2}$  ions are reduced by the polyol under the microwave radiation. The metallic cadmium reduces the selenium atom, and  $Zn^{+2}$  is incorporated into the formation of the crystalline selenide, by replacing a few  $Cd^{+2}$  ions in the unit cell. An additional control experiment for the preparation of the  $Cd_{1-x}Zn_xSe$  alloy is conducted also under acidic pH (<6) conditions. The  $Cd_{1-x}Zn_xSe$  is

**Table 2** Elemental analysis ratio for Cd:Zn of  $Cd_{1-x}Zn_xSe$  samples obtained from XPS measurements: (a) for  $Cd_{0.9}Zn_{0.1}Se$ ; (b) for  $Cd_{0.8}Zn_{0.2}Se$ ; (c) for  $Cd_{0.7}Zn_{0.3}Se$

| Theoretical Cd:Zn ratio | As-prepared samples | Heated samples |
|-------------------------|---------------------|----------------|
| (a) 0.9:0.1 = 9         | 9.09                | 9.80           |
| (b) 0.8:0.2 = 4         | 3.95                | 4.35           |
| (c) 0.7:0.3 = 2.33      | 2.30                | 2.59           |

not obtained in the acidic solution. This negative result substantiates our claim that  $Zn^{+2}$  ions are not reduced in the current reaction.

### Acknowledgements

Professor A. Gedanken thanks the German Ministry of Science through the Deutsche–Israel program (DIP) for supporting this research. The kind assistance of Dr Y. Gofer and Dr G. Salitra in the XPS measurements is gratefully acknowledged. The authors are also grateful to Professor Z. Malik of the Faculty of Life Science for extending the use of his facilities to us, to Professor W. Kaplan and Dr J. Josef of the Faculty of Material Engineering, Technion, for their assistance in HR-TEM measurements. O. P. thanks Y. Epstein for useful discussions.

### References

- 1 *Physics and Chemistry of II–VI Compounds*, ed. M. Aven and J. S. Prener, North Holland, Amsterdam, 1967.
- 2 S. T. Lakshmikumar, *Sol. Energy Mater. Sol. Cells*, 1994, **32**, 7; K. N. Raju, R. P. Vijayalakshmi, D. R. Reddy and B. K. Reddy, *J. Phys. Chem. Solids*, 1992, **53**, 341.
- 3 K. C. Sharma and J. C. Garg, *Indian J. Pure Appl. Phys.*, 1988, **26**, 480.
- 4 A. Hagfeldt and M. Gratzel, *Chem. Rev.*, 1995, **95**, 49.
- 5 W. H. Wang, Y. Geng, Y. Qian, M. R. Ji and X. M. Liu, *Adv. Mater.*, 1998, **10**, 1479.
- 6 V. Krishnan, D. Ham, K. K. Mishra and K. Rajeshwar, *J. Electrochem. Soc.*, 1992, **139**, 23; R. N. Bhattacharya and K. Rajeshwar, *Sol. Cells*, 1986, **16**, 237; G. Hodes, J. Manassen and D. Cahen, *Nature*, 1976, **261**, 403; B. Miller and A. Heller, *Nature*, 1976, **262**, 680.
- 7 G. M. Chow, K. L. Kurihara, D. Ma, C. R. Feng, P. E. Schoen and L. J. Martinez-Miranda, *Appl. Phys. Lett.*, 1997, **70**, 2315; F. Fiévet, J. P. Lagier and M. Figlarz, *MRS Bull.*, 1989, December, 29; M. S. Hegde, D. Larcher, L. Dupont, B. Beaudoin, K. Tekaia-Elhissien and J. M. Tarascon, *Solid State Ionics*, 1997, **93**, 33.
- 8 J. Li, Z. Chen, R. J. Wang and D. M. Prospero, *Coord. Chem. Rev.*, 1999, **190–192**, 707; J. Yang, S. H. Yu, X. L. Yang and Y. T. Qian, *Chem. Lett.*, 1999, 839.
- 9 H. S. Soliman, N. A. Ali and A. A. El-Shazly, *Appl. Phys. A*, 1995, **61**, 87.
- 10 O. Palchik, R. Kerner, J. Zhu and A. Gedanken, *J. Solid State Chem.*, 2000, **154**, 530; J. Zhu, O. Palchik, S. Chen and A. Gedanken, *J. Phys. Chem. B*, 2000, **104**, 7344; R. Kerner, O. Palchik and A. Gedanken, *Chem. Mater.*, 2001, **13**, 1413; O. Palchik, R. Kerner and A. Gedanken, *J. Solid State Chem.*, 2001, in press; O. Palchik, R. Kerner and A. Gedanken, *Chem. Mater.*, in press; J. Zhu, S. Liu, O. Palchik, Y. Kolytyn and A. Gedanken, *J. Solid State Chem.*, 2000, **153**, 342.
- 11 D. M. P. Mingos, *Res. Chem. Intermed.*, 1994, **20**, 85; D. M. P. Mingos, *Chem. Ind.*, 1994, 1 August, p. 596; D. R. Baghurst and D. M. P. Mingos, *J. Chem. Soc., Chem. Commun.*, 1992, 674; D. M. P. Mingos and D. R. Baghurst, *Chem. Soc. Rev.*, 1991, **20**, 1; S. Caddic, *Tetrahedron*, 1995, **51**, 10403.
- 12 A. G. Whittaker and D. M. P. Mingos, *J. Chem. Soc., Dalton Trans.*, 2000, 1521; A. G. Whittaker and D. M. P. Mingos, *J. Chem. Soc., Dalton Trans.*, 1995, 2073.
- 13 H. Grisaru, O. Palchik, A. Gedanken, V. Palchik, M. A. Slifkin, A. M. Weiss and Y. Rozenfeld Hacoheh, *Inorg. Chem.*, 2001, **40**, 4814.
- 14 P. Stadelmann, *Ultramicroscopy*, 1987, **21**, 131.
- 15 M. A. Slifkin, L. Luria and A. M. Weiss, *SPIE - Int. Soc. Opt. Eng., Proc.*, 1998, **3110**, 481.
- 16 *Photoacoustics and Photoacoustic Spectroscopy*, ed. A. Rosencawig, Academic Press, New York, 1980.
- 17 L. Samuel and Y. Brada, *Phys. Rev. B*, 1987, **36**, 1168; A. S. Nasibov, Y. V. Korostelin, P. V. Shapin, L. G. Suslin, D. L. Fedorov and L. S. Matkov, *Solid State Commun.*, 1989, **71**, 867.
- 18 *X-Ray Diffraction Procedures*, ed. H. Klug and L. Alexander, Wiley, New York, 1962, p. 125.
- 19 O. Palchik, R. Kerner, A. Gedanken, A. M. Weiss, M. A. Slifkin and V. Palchik, *J. Mater. Chem.*, 2001, **11**, 874.
- 20 H. C. Poon, Z. C. Feng, Y. P. Feng and M. F. Li, *J. Phys.: Condens. Matter*, 1995, **7**, 2783.

- 21 S. Gorer and G. Hodes, *J. Phys. Chem.*, 1994, **98**, 5338; S. A. Empedocles and M. G. Bawendi, *J. Phys. Chem. B*, 1999, **103**, 1826; B. Ludolph, M. A. Malik, P. O'Brien and N. Revaprasadu, *Chem. Commun.*, 1998, 1849.
- 22 J. F. Moulder, W. F. Stickle, P. E. Sobol and K. D. Bomben, in *Hand Book of X-Ray Photoelectron Spectroscopy*, ed. J. Chastain, Perkin Elmer, Eden Prairie, MN, 1992, ch. 3, p. 52.
- 23 A. P. Alavisatos, J. E. B. Katari and V. L. Colvin, *J. Phys. Chem. B*, 1994, **98**, 4109.
- 24 M. Figlarz, F. Fiévet and J. P. Lagier, *US Pat.*, 1985, 4,539,041; G. M. Chow, P. E. Schoen and L. K. Kurihara, *US Pat.*, 1998, 5,759,230.